The 2010 IEEE/RSJ International Conference on
Intelligent Robots and Systems
October 18-22, 2010, Taipei, Taiwan

Flocking of Micro-Scale Particles with Robotics and Optical Tweezers Technologies

Haoyao Chen, Jian Chen, Yanhua Wu, and Dong Sun

***Abstract*— This paper presents a novel flocking framework for the manipulation of micro-scale particles with robotics and optical tweezers technologies. A region-based flocking algorithm is used to calculate the particles' trajectories. The optical tweezers are used to trap and move the particles along generated trajectories. All particles can be gradually moved into a pre-defined region. The main contribution of this paper lies in the proposal of using multi-agent solution to address the flocking problem of particles in micro environment. The proposed framework can be applied to many bio-applications such as cell sorting, cell property characterization, and so on, with high throughput and precision. Experiments on micro-scale particles with a robot-tweezers system are finally performed to verify the effectiveness of the proposed approach.**

I. Introduction

Flocking is a form of collective phenomenon in which a large number of agents are organized into a coordinated motion. For many years, researchers from rather diverse fields, including animal behavior, social sciences, physics and biophysics, computer science, to some a few, have been fascinated by the behaviors of flocking/swarming/schooling in groups of agents [1]-[3]. Examples of these behaviors include flocking of birds, schooling of fish, and swarming of bacteria, etc. Recently, with the development of optical tweezers technology [4] and its application [5], flocking of micro-scale particles has attracted much attention among researchers in biology, medicine, materials science and possibly quantum computation [6]-[7]. Flocking of bio-particles has many advantages such as increasing throughput and improving statistics. For example, large array of beads coated with antibodies, and probe beads with a variety of antigens coated on the surface, can be flocked into two independent groups and then matched in batches.

H.Y. Chen is currently with the Department of Automation and Mechatronics at the Harbin Institute of Technology Shenzhen Graduate School, Shenzhen, China. He was with the Joint Advanced Research Centre of the City University of Hong Kong and the University of Science and Technology of China, Suzhou, China (Tel: 86-755-26033788; e-mail: hychen5@mail.ustc.edu.cn).

J. Chen is with the Department of Manufacturing Engineering and Engineering Management, City University of Hong Kong, Kowloon, Hong Kong (e-mail: lixiang@mail.ustc.edu.cn).

Y.H. Wu is with the Mechanics and Automation Group, Suzhou Research Center of City University of Hong Kong and University of Science and Technology of China, Suzhou, China (e-mail: wuyhok@mail.ustc.edu.cn).

D. Sun is with the Department of Manufacturing Engineering and Engineering Management, City University of Hong Kong, Kowloon, Hong Kong (Tel: 852 27888405; e-mail: medsun@cityu.edu.hk).

Many methods inspirited from natural flocking behavior have been developed for engineering applications especially in robotics in the past two decades [19]. Reynolds [1] proposed a classical flocking model consisting of three heuristic rules: flocking centering, obstacle avoidance, and velocity matching. Based on these rules, Olfati-Saber [8] utilized graph theory and artificial potentials to investigate the consensus problem of multiple simulated particles. Flocking in both free-space and obstacle-space were investigated. Simulations were proposed to illustrate the effectiveness of the algorithm. Leonard *et al.* [9] presented a framework for coordinated and distributed control of multiple autonomous vehicles using artificial potentials and virtual leaders. This framework allows for a homogeneous group without ordering of vehicles. Several simulations were proposed to verify the stability results. Cheah *et al.* [10] developed a region-based shape controller for a swarm of robots. Robots move as a group inside a desired region while maintaining a minimum distance among themselves. Various shapes of the desired region can be formed by choosing appropriate objective functions. A Lyapunov-like function is presented for convergence analysis of the system. Sun *et al.* [11] proposed a synchronization control approach for formation control, which is a special example of flocking control. The major idea is to control robots to track each desired trajectory individually while synchronizing the motions amongst the robots to maintain relative kinematics relationship as required by the formation.

Most of previous flocking approaches were developed for applications in macro environments, and few of them have been found in automatic flocking of micro-scale particles in micro environments. Korda *et al.* [12] reported the measurement of colloidal transporting through arrays of micrometer-scale potential wells created with *holographic optical tweezers* (HOT) [13]. But the method could not transport distributed colloidal particles to the wells automatically. Arai *et al.* [6] developed an integrated optical tweezers system, and proposed a generalized phase contrast method for trapping multiple particles simultaneously. A demonstration of trapping 36 polystyrene beads to form a rectangular shape manually was also presented. Chapin *et al.* [7] presented a method for forming particles, where a destination was assigned to each particle manually, and a simple set of traffic rules were proposed to transform an arbitrary initial configuration of trapped particles to the

desired configuration.

In this paper, we propose a control framework for the manipulation of micro-scale particles with integration of robotics and *HOT* technologies. With this framework, particles can be trapped individually by *HOT*, moved to a desired region, and arrayed regularly. The main contribution of this paper lies in the proposal of using multi-agent solution to address the flocking problem of particles in micro environments. The approach is two-fold. First, a region-based flocking control algorithm [10] for macro robotic applications is adopted in our approach to calculate particles' trajectories automatically, along which micro-scale particles are trapped by optical tweezers without any collision. Second, a visual servo feedback scheme, containing a multi-particle detecting process, is proposed to offer the position information of particles for the flocking control.

II. Flocking Control of Micro-scale Particles With Holographic Optical Tweezers

A. Operation with Holographic Optical Tweezers

The optical forces exerted by a few milli-Watts of laser light can dominate the dynamics of nano- and micro-particles. Optical tweezers exploit these forces to precisely manipulate particles or cells without mechanical contact. Trapping of a micro particle is achieved by focusing a laser beam on it, which can be further extended to multiple traps using holography. Fig. 1 shows a robotic manipulation setup that is equipped by a holographic optical tweezers system (BioRyx 200, Arryx) in City University of Hong Kong, which includes an executive module, a sensory module, and a control module. The *executive module* consists of an X-Y-Z motorized stage (ProScan, Prior Scientific) with microscopic objectives mounted on the Z-axis and a holographic optical trapping device (HOT). Biological samples are contained in a home-built chamber, which is placed on the two-dimensional X-Y motorized stage with a positioning accuracy of 15 *nm*. The *sensory* module includes an inverted microscope (Nikon TE2000, Japan), a CCD camera (FO124SC, Foculus), and a PCI image capture and processing card. The positions of the biological objects can be obtained through image processing, which serves as visual feedback to guide the micromanipulation process. The *control module* consists of a motion controller for X-Y-Z motorized stage [18], a phase modulator for HOT device, a stepping motor controller for the spot moving of laser scissor, and a host computer. All of the mechanical components were supported upon an anti-vibration table. In the optical tweezers, a continuous wave (CW) laser beam (V-106C-3000 OEM J-series, Spectra Physics) with wavelength of 1064 *nm* is sculpted by the HOT device and up to 200 optical traps can be created simultaneously. These traps serve as microtools to manipulate multiple micro/nano-scale particles with size ranged from 100 *nm* to 100 μm.

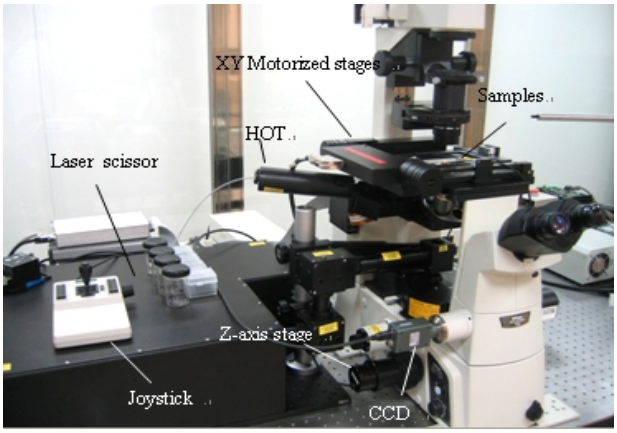

(a) Experimental setup.

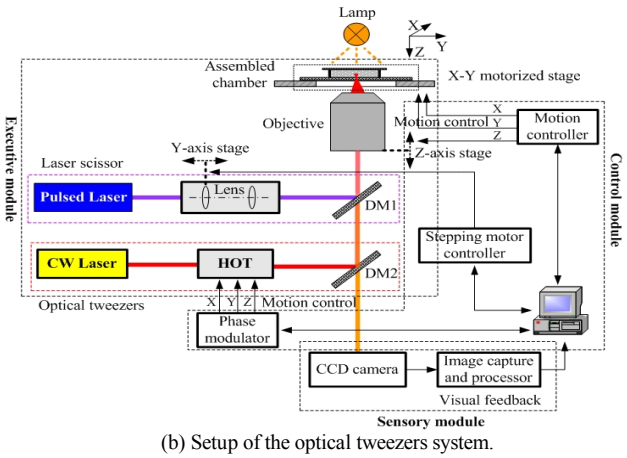

(b) Setup of the optical tweezers system.

Fig. 1. Cell manipulation system with optical tweezers.

B. The region-based Flocking Control Algorithm for Micro-scale Particles

Colloidal silica particles are selected in our manipulation experiments, since it is easier to be obtained and reposited than other micro-scale particles. The dielectric particles can be precisely manipulated based on *HOT,* which further enables delicate mechanical measurement at the molecular and colloidal scales [7]. In fact, the presented framework can be used not only for the flocking control of silica particles, but also for easy extension to other biological particles or live cells, e.g., saccharomycetes, and erythrocytes, etc. Since all silica particles are suspending in the water solution, they can be trapped and moved to any direction in the X-Y plane by using optical tweezers. Therefore, silica particles can be treated as omni-driven agents in 2D space [14], and the dynamics of the i^{th} particle can be described as:

$$\begin{cases} \dot{X}_i = V_i \\ \dot{V}_i = U_i \end{cases} \tag{1}$$

where $X_i = [x_i, y_i]^T \in R^2$ is the position vector, $V_i = [V_{x_i}, V_{y_i}]^T \in R^2$ denotes the velocity vector, and $U_i \in R^2$ denotes the control input.

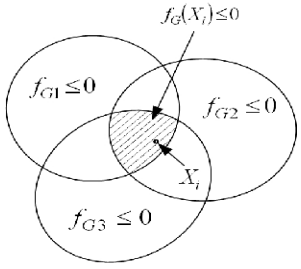

Fig. 2. Example of the global objective function $f_G(X_i)$.

As shown in Fig. 2, any desired region (the shadow region) can be mathematically described as a global objective function intersected by a set of constraint regions. The function is defined by the following inequality

$$f_G(X_i)=\{f_{G1}(\Delta X_{io1}),f_{G2}(\Delta X_{io2}),\cdots,f_{GM}(\Delta X_{ioM})\}^T\le 0 \quad (2)$$

where $f_{Gm}(\cdot)\le 0 \ \ (m=1,2,\cdots M)$, denoting a number of constraint regions, and M is the total number; $\Delta X_{iom}=X_i-X_{om}$ denotes the position difference, $X_{om}(t)=[x_{om},y_{om}]^T$ is a reference position within the m^{th} constraint region $f_{Gm}(\Delta X_{iom})\le 0$. Note that $f_{Gm}(\Delta X_{iom})$ are continuous scalar functions with continuous partial derivatives with respect to ΔX_{iom}. The inequality $f_G(X_i)\le 0$ indicates that particle i stays in the intersection region of all the M constraint regions. For micro physical applications, such as sorting, transition, and parallel processing of particles, particles are often transited into a rectangular region [7]. In this paper, only the rectangular shape case is considered. Other shapes can also be implemented by selecting correct objective functions. A rectangular shape can be formed by choosing the objective functions as follows:

$$\begin{cases} f_{G1}(\Delta X_{io1})=a^2/4-(x_i-x_{o1})^2\le 0 \\ f_{G2}(\Delta X_{io2})=b^2/4-(y_i-y_{o2})^2\le 0 \end{cases} \quad (3)$$

where a and b are constants, i.e., the width and height of the desired rectangular, $\Delta X_{io1}=\Delta X_{io2}$, and $[x_{o1}=x_{o2},\ y_{o1}=y_{o2}]$ denotes the reference point, i.e. the rectangular center.

Colloid particles cannot be too close with each other, or they will bind together and are not easy to be separated. Therefore, a minimum distance between two particles should be specified. This relationship can be represented as a local objective function by the following inequality:

$$g_{Lij}(\Delta x_{ij})=d^2-\left\|\Delta X_{ij}\right\|^2\le 0 \quad (4)$$

where $\left\|\Delta X_{ij}\right\|=\left\|X_i-X_j\right\|$ is the Euclidean distance between particle i and j, and d is a minimum distance between the two particles.

By defining a global objective function and a local objective function, the group of particles is required to move in a desired shape while maintaining a minimum distance among each other.

The potential energy of the global objective function (3) involving the i^{th} particle, which is also called attractive potential, is calculated as follows:

$$P_{Gi}(\Delta X_{io1})=\frac{k_1}{2}(\max(0,f_{G1}(\Delta X_{io1})))^2+\frac{k_2}{2}(\max(0,f_{G2}(\Delta X_{io2})))^2 \quad (5)$$

where k_1 and k_2 are positive constants. Meanwhile, the potential energy of the local objective function (4), i.e., the repulsive potential, is defined as:

$$Q_{Lij}(\Delta X_{ij})=\sum_{j\in N_i}\frac{k_{ij}}{2}(\max(0,g_{Lij}(\Delta X_{ij})))^2 \quad (6)$$

where k_{ij} is positive constant, and N_i denotes a set of neighbors around particle i. Given an interaction range $r_N>d$, any particle that is at a distance smaller than r_N from particle i is called a neighbor of particle i.

The gradient $\Delta\xi_i$ of the function (5) represents its partial differential with respect to ΔX_{io1}, which is defined as:

$$\begin{aligned}\Delta\xi_i&=\frac{\partial P_{Gi}(\Delta X_{io1})}{\partial\Delta X_{io1}}\\&=k_1(\max(0,f_{G1}(\Delta X_{io1})))\left(\frac{\partial f_{G1}(\Delta X_{io1})}{\partial\Delta X_{io1}}\right)^T\\&\quad+k_2(\max(0,f_{G2}(\Delta X_{io1})))\left(\frac{\partial f_{G2}(\Delta X_{io1})}{\partial\Delta X_{io1}}\right)^T\end{aligned} \quad (7)$$

Note that when the particle is outside the desired region, the gradient force $\Delta\xi_i$ is activated to attract the particle i toward the desired region. When the particle is inside the desired region, then $\Delta\xi_i=0$.

Partially differentiating (6) with respect to ΔX_{ij}, we have

$$\begin{aligned}\Delta\rho_{ij}&=\frac{\partial Q_{Lij}(\Delta X_{ij})}{\partial\Delta X_{ij}}\\&=\sum_{j\in N_i}k_{ij}(\max(0,g_{Lij}(\Delta X_{ij})))\left(\frac{\partial g_{Lij}(\Delta X_{ij})}{\partial\Delta X_{ij}}\right)^T\end{aligned} \quad (8)$$

The control force $\Delta\rho_{ij}$ is activated only when the distance $\left\|\Delta X_{ij}\right\|$ is smaller than the minimum distance d. When particle i maintains the minimum distance d to its neighboring particles, $\Delta\rho_{ij}=0$.

Further, define a vector $\dot{X}_{ri}$ as

$$\dot{X}_{ri}=\dot{X}_{o1}-\alpha_i\Delta\xi_i-\gamma\Delta\rho_{ij}=\dot{X}_{o1}-\Delta\varepsilon_i \quad (9)$$

where α_i and γ are positive constants, $\dot{X}_{o1}$ denote the velocity vector of the region center, and

$$\Delta\varepsilon_i=\alpha_i\Delta\xi_i+\gamma\Delta\rho_{ij} \quad (10)$$

denotes a combined force of the attractive and repulsive potential force defined in (7) and (8). When particle i maintains a minimum distance to all of its neighboring particles inside the desired region, $\Delta\varepsilon_i$ =0. A sliding vector for particle i is then defined as

$$s_i = \dot{X}_i - \dot{X}_{ri} = \Delta\dot{X}_{io1} + \Delta\varepsilon_i \tag{11}$$

where $\Delta\dot{X}_{io1} = \dot{X}_i - \dot{X}_{o1}$. The derivative of s_i with respect to time is

$$\dot{s}_i = \ddot{X}_i - \ddot{X}_{ri} = \Delta\ddot{X}_{io1} + \Delta\dot{\varepsilon}_i \tag{12}$$

where $\ddot{X}_{ri} = \ddot{X}_{o1} - \Delta\dot{\varepsilon}_i$. Substituting (12) into Eq. (1), we have

$$\dot{s}_i + \ddot{X}_{ri} = U_i \tag{13}$$

It can be seen that $\ddot{X}_{ri}$ is treated as a known regressor matrix [14].

Based on (7)-(13), the rectangular shape controller for a swarm of particles is proposed as:

$$U_i = -K_{s_i} s_i - K_p \Delta\varepsilon_i + \ddot{X}_{ri} \tag{14}$$

where K_{si} and K_p are positive definite control gain matrices.

Theorem 1: Consider a group of n particles with dynamics described by equation (1). The control law (14) gives rise to $\Delta\varepsilon_i \to 0$ and $\Delta\dot{X}_i \to 0$ for all $i = 1,2,\cdots,n$, as $t \to \infty$.

Proof: For the detailed proof, please refer to [10].

When using optical tweezers systems, the physical limitation of velocity should be considered [15]. The finite spatial extent of the optical trap limits the step size, denoted by *h*, between successive trap locations. Subsequently, the speed of trapped particles is limited within *hf*, where *f* is the refresh rate of the feedback loop. With faster feedback loops, the maximum velocity is ultimately determined by the balance of viscous and optical forces on the trapped particles. In our system, all the particles are trapped within a constant area of the field of view of the microscope, so the maximum velocity can be guaranteed by bounding the maximum acceleration of the motion of the optical tweezers, i.e., bounding the control inputs U_i. Therefore, the parameters of K_{si} and K_p should be set small enough to make sure that the optical tweezers can trap the particles successfully.

Further, to guarantee the control input not to exceed a maximum acceleration, the controller (14) can be revised by utilizing a saturation control method as follows:

$$sat(U_i) = \begin{cases} -K_{s_i} s_i - K_p \Delta\varepsilon_i + \ddot{X}_{ri}, & \|U_i\| < k \\ k \dfrac{-K_{s_i} s_i - K_p \Delta\varepsilon_i + \ddot{X}_{ri}}{\left\| -K_{s_i} s_i - K_p \Delta\varepsilon_i + \ddot{X}_{ri} \right\|}, & \|U_i\| \geq k \end{cases} \tag{15}$$

where $U_i = -K_{s_i} s_i - K_p \Delta\varepsilon_i + \ddot{X}_{ri}$, and k denotes a factor about the maximum acceleration. The maximum acceleration is detailed discussed in [15]. Based on the experiments, the value k is generally set to $0 < k < 1$, where the bigger value indicates faster convergence rate. When K_{si} and K_p are constant, only one parameter k needs to be modified for different particles and solutions. As a result, the parameter selection of controller (15) is much easier than the controller (14). In our experiments, we found that only bounding the control input is not enough. Sometimes the velocity may grow greatly. Thus, we further set the velocity as $V_i = \dot{X}_i \equiv 0$, which means that the flocking always starts at zero states in every process loop, and thus, we do not need to consider the convergence of $\Delta\dot{X}_i$. This feature makes sure that the controlled system is stable. The controller (15) is then simplified as

$$sat(U_i) = \begin{cases} -K_{s_i}(-\dot{X}_{o1} + \Delta\varepsilon_i) - K_p \Delta\varepsilon_i + \ddot{X}_{ri}, & \|U_i\| < k \\ k \dfrac{-K_{s_i}(-\dot{X}_{o1} + \Delta\varepsilon_i) - K_p \Delta\varepsilon_i + \ddot{X}_{ri}}{\left\| -K_{s_i}(-\dot{X}_{o1} + \Delta\varepsilon_i) - K_p \Delta\varepsilon_i + \ddot{X}_{ri} \right\|}, & \|U_i\| \geq k \end{cases} \tag{16}$$

where $U_i = -K_{s_i}(-\dot{X}_{o1} + \Delta\varepsilon_i) - K_p \Delta\varepsilon_i + \ddot{X}_{ri}$.

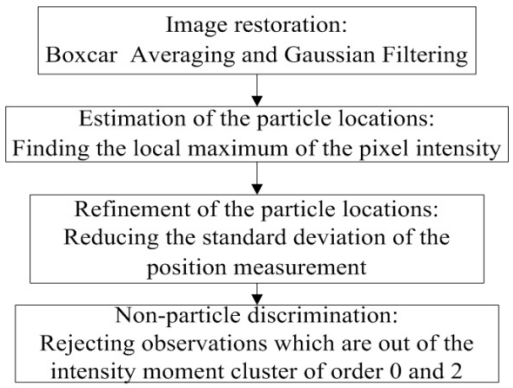

Fig.3. The flow of the particle detection.

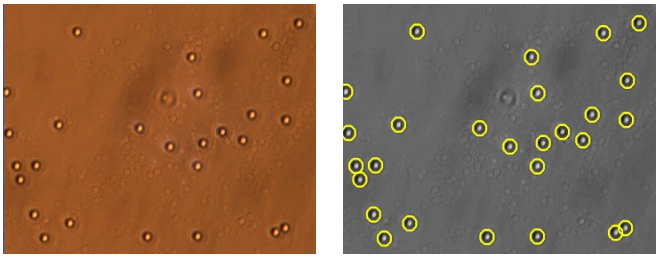

(1) Source image (2) Detection results

Fig. 4. Example of particle detection process.

III. Multi-Particle Detection and Flocking Control Framework

The positions of particles are detected by processing sequential images captured by the microscope camera. The well-known particle tracking algorithm [16], [17] is utilized to process the images. The algorithm consists of two main parts: particle location detection and particle tracking. In this paper, we assume that every trapped particle can be tightly trapped by the optical tweezers, and thus the time-consuming particle tracking can be omitted. Fig. 3 illustrates four sub-steps of the particle location detection. Fig. 4 shows an example of the particle detection. The source image is captured by the camera of the optical tweezers system as

shown in Fig. 1. Although the source image has much noise, all true particles labeled with small circles are detected successfully, as shown in Fig. 4. Furthermore, the sub-pixel accuracy of detection can be achieved.

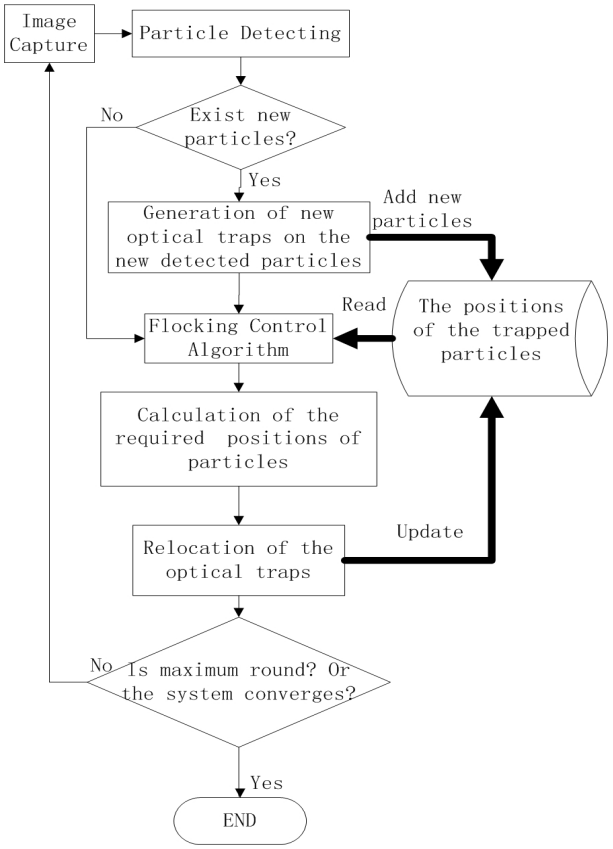

Fig. 5. The flow of the flocking control framework.

Based on the flocking control algorithm and the particle detecting algorithm, the flow chart of flocking of micro-particles manipulated by optical tweezers is shown in Fig. 5. There are three main steps in the process.

1) Detecting non-trapped particles. Once the particles are detected, comparison between positions of the detected particles and trapped particles is done to check whether there exist non-trapped particles. An optical trap is generated on each new particle, which is then labeled as a trapped particle and stored in database with its current position.

2) Calculating destinations of particles. The current positions in database are utilized to calculate the control input U_i for the i^{th} trapped particle by using the flocking control algorithm. Based on the dynamic model (1), the required positions are then calculated as

$$X_i(t+T) = X_i(t) + \frac{1}{2}U_i T^2 \tag{17}$$

where t is the current time, and T denotes the interval time of each loop. The trapped particles are then moved to their respective destinations by relocating positions of the optical traps. Finally, positions of all trapped particles in database are updated.

3) Loop checking. To automatically stop the flocking process, a force variable is defined as

$$\Delta\varepsilon = \frac{1}{n}\sum_{i=1}^{n}\sqrt{\Delta\varepsilon_i^T \Delta\varepsilon_i} \tag{18}$$

where $\Delta\varepsilon_i$ is defined in (10). If $\Delta\varepsilon < \Delta\varepsilon_{\min}$, where $\Delta\varepsilon_{\min}$ is the minimum force, the flocking of the system is treated to reach a stable state. When $\Delta\varepsilon < \Delta\varepsilon_{\min}$ or the maximum loop count is reached, the flocking process stops.

IV. Experiments

Experiments were performed on the established cell manipulation system (Fig.1) to demonstrate the effectiveness of the proposed flocking approach. Silica micro-scale particles with the size of $2\mu m$ were selected, and dissolved into water solution. Particle images were captured using a CCD camera (640×480 pixels) under 40X microscope. For the BioRyx 200 optical tweezers, positions of any optical traps must not exceed the diffractive element device (DED) coordinate range (512×512). Therefore, a calibration is needed to map a 640×480 particle image to the diffractive element device by using following equations

$$\begin{cases} x_d = \dfrac{x_I}{640}\times 512 \\ y_d = \dfrac{y_I}{480}\times 512 \end{cases} \tag{18}$$

where $[x_d, y_d]^T$ and $[x_I, y_I]^T$ denote the positions with respect to the DED frame and image frame, respectively.

Further, the desired rectangular shape was specified with $a = 120/600$, $b = 100/600$. The minimum distance d was set to 50/600, and the interaction range r_N was set to 350/600. X_{o1} was set to $[320,240]^T/600$, $\dot{X}_{o1} = 1/600$, and $\ddot{X}_{o1} = 0$. Note that all the units of variables were set to (600pixel). The control gains were set as $k = 0.4$, $K_{si} = diag\{30,30\}$, $K_p = diag\{1,1\}$, $k_{ij} = 1$, $k_1 = k_2 = 1$, $\gamma = 150$, and $\alpha_i = 70$. The time interval T of each loop was set to 150ms and the minimum error $\Delta\varepsilon_{\min}$ was set to 0.025.

Fig. 6 shows positions of all the particles at various time instances. The particles are indicated with circles, and numbered sequentially. The index number of each particle keeps the same over the whole process. As can be seen in Fig. 6, seven particles were detected at time 0s, and were gradually moved into the desired rectangular. At time 15s and 19s, two new particles were detected and added into the flocking process. Finally all these nine particles were moved into the rectangular to form a regular array. Fig. 7 illustrates the force variable $\Delta\varepsilon$ with respect to time. It can be seen that the force gradually converges to zero, which indicates that the flocking reaches a stable state.

V. Conclusions

In this paper, a flocking control approach using robot-tweezers manipulation system is proposed for a group

of micro-scale particles in micro environments. A region-based algorithm and a visual servo control scheme are integrated into the system to achieve the flocking of micro-scale particles. Experiments on optical tweezers system are performed to verify the effectiveness of the presented framework. The future work includes studies on improving the convergence rate of the algorithm and flocking experiments on swarms of particles.

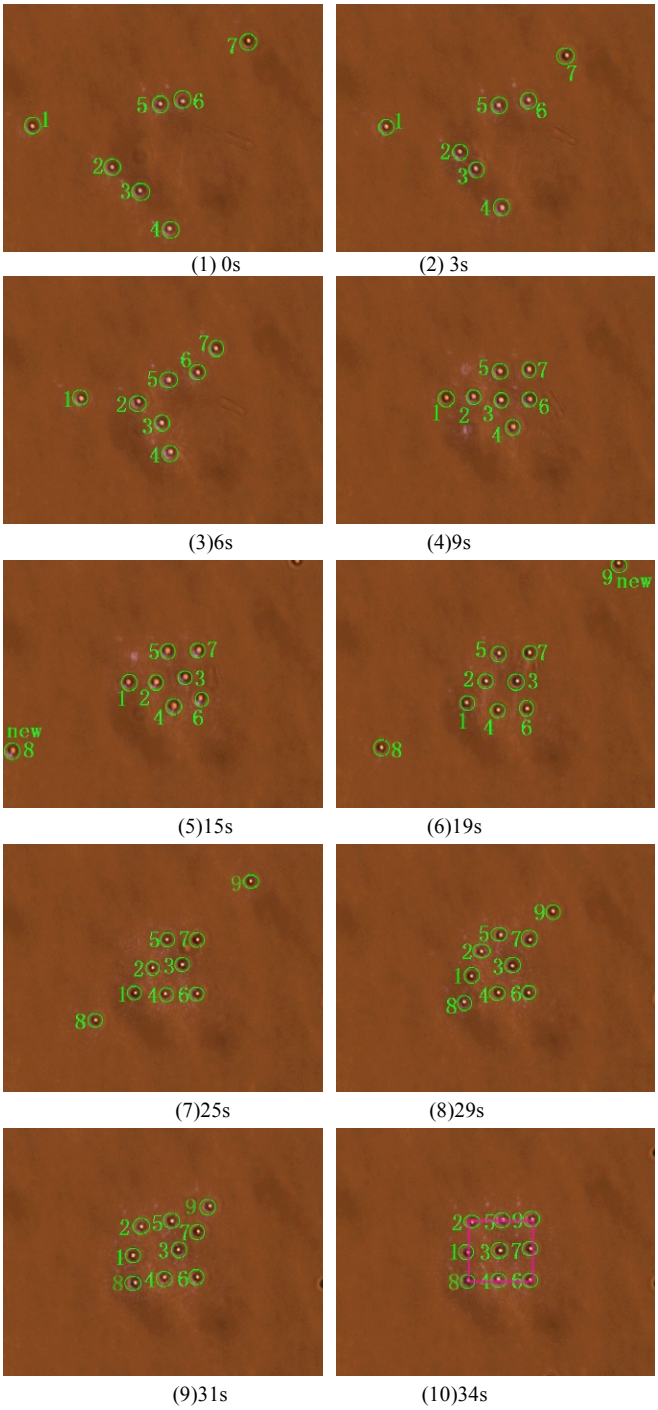

Fig. 6. Snapshots of the flocking experiment of multiple silica particles with optical tweezers.

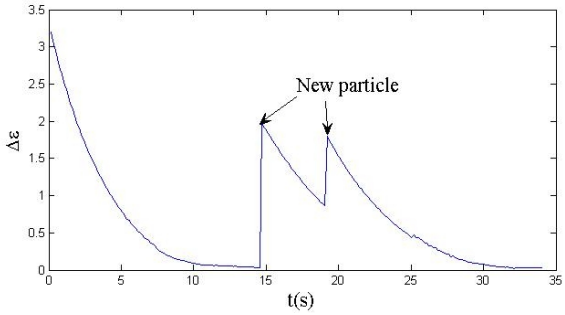

Fig. 7. The value of $\Delta\varepsilon$ with respect to time.

REFERENCES

[1] C. Reynolds, "Flocks, heads and schools: A distributed behavioral model," *Computer Graphics*, vol.21, pp.25-34, 1987.

[2] Shaw, "Fish in schools," Natural History, vol.84, no.8, pp.40-45, 1975.

[3] H. Levine and W. J. Rappel, "Self organization in systems of self-propelled particles," *Phys. Rev. E*, vol.63, pp.208-211, 2001.

[4] A. Ashkin, J. M. Dziedzic, J. E. Bjorkholm, and S. Chu, "Observation of a single-beam gradient force optical trap for dielectric particles," Optics Letters, vol. 11, no. 5, pp.288, 1986.

[5] Y. Tan, D. Sun, J. Wang, and W. Huang, "Mechanical characterization of human red blood cells under different osmotic conditions by robotic manipulation with optical tweezers," *IEEE Trans. on Biomedical Engineering*, vol. 57, no. 7, pp. 1816-1825, July 2010.

[6] F. Arai, K. Onda, R. Iitsukam, and H. Maruyamam, "Multi-beam Laser Micromanipulation of Micro-tool by Integrated Optical Tweezers," *in Proc. of ICRA 2009*, Japan, May, 2009.

[7] S. C. Chapin, V. Germain, and E. R. Dufresne, "Automated trapping, assembly, and sorting with holographic optical tweezers," *Optics Express*, vol. 14, no. 26, pp. 13095-13100, 2006.

[8] R. Olfati-Saber, "Flocking for multi-agent dynamic systems: Algorithms and Theory," *IEEE Trans on Automatic Control*, vol.51, no.3, pp. 401-420, 2006.

[9] N. Leonard, and E. Friorelli, "Virtual leaders, artificial potentials and Coordinated control of groups," in *Proc. 40th IEEE Conf. Decision Control*, Orlando, FL, pp. 2968-2973, Dec. 2001.

[10] C. C. Cheah, S. P. Hou, J. J. E. Slotine, "Region-based shape control for a swarm of robots," *Automatica*, vol.45, pp.2406-2411,2009.

[11] D. Sun, C. Wang, W. Shang, and G. Feng, "A synchronization approach to trajectory tracking of multiple mobile robots while maintaining time-varying formations," *IEEE Trans. on Robotics*, vol. 25, no. 5, pp.1074-1086, 2009.

[12] P. T. Korda, M. B. Taylor, and D. G. Grier, "kinetically locked-in colloidal transport in an array of optical tweezers," *Physical review letters*, 2002.

[13] E. R. Dufresne, G. C. Spalding, M. T. Dearing, S. A. Sheets, and D. G. Grier, "Computer-generated Holographic Optical Tweezer Arrays," *Rev Sci Instrum*, vol.72, pp.1810, 2001.

[14] J. J. E. Slotine, and W. Li, "Applied nonlinear control," Englewood Cliffs, New Jersy: Prentice Hall.

[15] Y. Wu, Y. Tan, D. Sun, and W. Huang, "Force Analysis and Path Planning of the Trapped Cell in Robotic Manipulation with Optical Tweezers," *IEEE Int. Conf. on Robotics and Automation,* Ancorage, AL, pp.4119-4124, 2010.

[16] J. C. Crocker, and D. G. Grier, "Methods of Digital Video Microscopy for Colloidal Studies,"*J. Colloid Interface Sci*. vol.179, pp. 298, 1996.

[17] I. F. Sbalzarini, and P. koumoutsakos, "Feature point tracking and trajectory analysis for video imaging in cell biology," *Journal of Structural biology*, vol.151, pp.182-195, 2005.

[18] D. Sun, J. B. Liu and X. Ai, "Modeling and performance evaluation of traveling-wave piezoelectric ultrasonic motors with analytical method," *Sensors and Actuators: A Physical*, vol. 100, no. 1, pp. 84-93, Oct. 2002.

[19] H. Y. Chen, D. Sun, J. Yang, and J. Chen, "SLAM Based Global Localization for Multi-robot Formations in Indoor Environment," *IEEE/ASME Trans. on Mechatronics*, vol. 15, no. 4, 2009